Reduced warp in torsion of reticulated foam due to Cosserat elasticity: experiment

Roderic S. Lakes

May 25, 2016

Department of Engineering Physics, Department of Materials Science
University of Wisconsin, 1500 Engineering Drive, Madison, WI 53706-1687, USA

preprint adapted from Lakes, R. S., Reduced warp in torsion of reticulated foam due to Cosserat elasticity: experiment, Zeitschrift fuer Angewandte Mathematik und Physik (ZAMP), 67(3), 1-6 (2016).

Abstract

Warp of cross sections of square section bars in torsion is reduced in Cosserat elasticity in comparison with classical elasticity. Warp is observed experimentally to be substantially reduced, by about a factor of four compared with classical elasticity, in an open cell polymer foam for which Cosserat elastic constants were previously determined. The observed warp in the foam is consistent with a prediction based on Cosserat elasticity. Concentration of strain in the foam is therefore reduced in comparison with classical elasticity.

1 Introduction

For torsion of a square section classically elastic bar, warp of cross sections occurs [1]. The warp, for torsion about the z axis, is

$$u_z = \theta[xy - \sum_{n=0}^{\infty} B_n sinh(k_n y) sin(k_n x)] \tag{1}$$

in which $k_n = (2n+1)\pi/a$ and $B_n = 8(-1)^n/ak_n cosh(k_n a/2)$, a is the bar width, and θ is twist angle per length. The twist displacements are

$$u_x = -\theta yz \tag{2}$$

$$u_y = \theta xz \tag{3}$$

The maximum warp deformation is $u_z^{max} = 0.037\theta a^2$. The warp is associated with a concentration of strain: the strain is maximum at the centerline of each free surface and zero at the edges. The maximum shear strain is given in terms of the twist angle (in radians) per unit length as $\gamma_{shear} = \theta a[1 - 0.4(8/\pi^2)] = 0.68\theta a$. The tensorial shear ϵ_{xz} is half of that. Foams and other materials with microstructure have a structural length scale but classical elasticity contains no length scale in the continuum view. The Cosserat theory of elasticity, by contrast, does incorporate a length scale.

The Cosserat theory of elasticity [2] [3] incorporates a local rotation of points as well as the translation of points in classical elasticity; also a couple stress (a torque per unit area) as well as the force per unit area defined as stress in classical elasticity. Cosserat elasticity is of interest in the context of stress concentrations. For example, the stress concentration factor for a circular hole is smaller than the classical value [4]. The equations for linear isotropic Cosserat (micropolar) elasticity are as follows [5].

$$\sigma_{ij} = 2G\epsilon_{ij} + \lambda\epsilon_{kk}\delta_{ij} + \kappa e_{ijk}(r_k - \phi_k) \tag{4}$$

$$m_{ij} = \alpha\phi_{k,k}\delta_{ij} + \beta\phi_{i,j} + \gamma\phi_{j,i} \tag{5}$$

The stress σ_{jk} in Cosserat elasticity can be asymmetric. The distributed moment from this asymmetry is balanced by a couple stress m_{jk} (a torque per unit area). ϕ_m is the rotation of points, called micro-rotation, e_{jkm} is the permutation symbol, and $r_k = \frac{1}{2}e_{klm}u_{m,l}$ is "macro" rotation based on the antisymmetric part of gradient of displacement u_i. Elastic constants G and λ have the same meaning as in classical elasticity; α, β, γ, and κ are Cosserat constants. Technical Cosserat elastic constants are defined as follows.

$$Young's\ modulus \qquad E = \frac{G(3\lambda + 2G)}{\lambda + G} \tag{6}$$

$$Shear\ modulus \qquad G \tag{7}$$

$$Poisson's\ ratio \qquad \nu = \frac{\lambda}{2(\lambda + G)} \tag{8}$$

$$Characteristic\ length,\ torsion \qquad \ell_t = \sqrt{\frac{\beta + \gamma}{2G}} \tag{9}$$

$$Characteristic\ length,\ bending \qquad \ell_b = \sqrt{\frac{\gamma}{4G}} \tag{10}$$

$$Coupling\ number \qquad N = \sqrt{\frac{\kappa}{2G + \kappa}} \tag{11}$$

$$Polar\ ratio \qquad \Psi = \frac{\beta + \gamma}{\alpha + \beta + \gamma}. \tag{12}$$

Warp of cross sections is reduced in Cosserat elasticity [6] in comparison with classical elasticity for a bar of square cross section in torsion. In a Cosserat solid, strain spills over into the corner region where classically stress and strain are zero; peak strain, hence strain concentration, is reduced in comparison with the prediction of classical elasticity. Reduction in warp [7] and evidence of corner strain [8] has been observed in dense foams. In these materials, the Cosserat coupling number N is small, 0.2 for dense closed cell polyurethane foam [9] and about 0.2 (range 0.1 to 0.3) for closed cell polymethacrylamide foam [10] as determined from size effects. Size effects also enabled determination of the Cosserat characteristic length in a two dimensional polymer honeycomb [11] but warp is a three dimensional phenomenon. On a much smaller scale, asymmetric interatomic interaction was analyzed in magnetic materials; non-central force was demonstrated with electron paramagnetic resonance [12] and interpreted in the context of Cosserat elasticity. Warp of a bar 16.6 mm in square cross section polymethacrylamide foam (cell size about 0.65 mm) was reduced to 80% of its classical value as determined by holographic interferometry [7]. The modest reduction in warp is associated with the small value of the Cosserat coupling number N.

The reason for the reduction in warp is easy to visualize. In classical elasticity, the stress at the corner of the square cross section must be zero because a corner differential element has two free surfaces that undergo zero shear stress and the stress is symmetric. So, the strain must be zero as well. Because the bar is twisted there must be shear strain somewhere, specifically in regions away from the corners. Therefore there must be warp. In Cosserat elasticity, the stress can be asymmetric, with the resulting moment balanced by a couple stress. Then the stress and strain at the corners of the cross section can be nonzero, allowing reduced warp as revealed by analysis [6].

Strong warp reduction effects are predicted to occur in a single specimen even if it is much larger than the characteristic length provided the coupling number N is large, approaching its upper limit 1. For low density reticulated foam, N as large as 0.99 has been inferred from size effects in torsion [13], so the reduction in warp should be substantial. In the present study, warp in torsiondigital is examined in this open cell foam.

2 Experimental methods

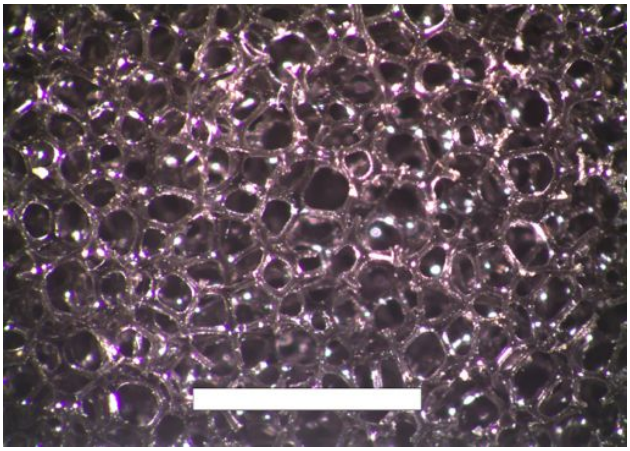

Figure 1: Foam structure; visible light micrograph. Scale mark 3 mm.

Polymer open cell reticulated foam (Scott Industrial foam [14]) was studied. The foam was specified as 60 pores per inch (60 ppi) corresponding to a cell size of 0.4 mm. The structure is shown in Figure 1. Cosserat constants were determined from size effects in torsion [13] to be ℓ_t = 1.6 mm, N = 0.99, Ψ = 1.5. A specimen of solid rubber was also studied for comparison as a classically elastic material. Both specimens were 25 mm square.

Torsion was achieved by cementing each end of the specimen to a calibrated micrometer driven rotation stage (Newport type 472). The stages were fixed to an optical breadboard (Thorlabs type 273). Each stage was rotated an equal amount in opposite directions to achieve torsion with minimal displacement near the center. Digital images of the center region were taken before and after deformation. Deformation was determined with digital image superposition and with digital image correlation. For the image superposition approach, images were taken using a 7 megapixel Olympus camera. Initial images were taken of the foam surface before and after deformation. Then rubber markers about 1.5 mm wide were glued to the specimen and further images before and after deformation were captured. Images were color coded and superposed; deformation was measured using GIMP image processing software. In both methods, tilt motion (a linear function) and rigid motion (a constant) were subtracted to obtain the warp.

For digital image correlation, the reflectivity of the foam surface was increased with a thin coating of chalk dust. Oblique light was used to illuminate the surface. The purpose was to minimize light penetration into the foam so that only the surface layer is analyzed. It was helpful that the foam was dark gray. A Correlated Solutions VIC 2D system on a Dell computer was used. This method requires a speckle pattern upon the object [15] [16]. For stiff specimens this pattern is usually obtained by spray paint on the surface. For foam, the cell heterogeneity was used. It is known that the natural surface of polymer foam provides sufficient contrast to compute reliable correlations [17]. For rubber, fine scratches were made with a probe on the surface to provide a pattern of contrast. For a 86 mm long foam specimen subjected to a $\pm 6^\circ$ twist for image correlation, the maximum classical warp was 67 μm and the maximum classical shear strain was ϵ_{xz} = 0.021. This is well within the linear range for this type of foam. More twist, $\pm 17^\circ$ on a 95 mm long specimen, was used for photographic image superposition to obtain sufficient resolution; the corresponding classical peak strain was 0.053, also within the linear range. Warp displacement was captured via image correlation in several line scans in the transverse direction. Warp displacement was also captured along axial line segments and was averaged to generate experimental data points.

3 Results

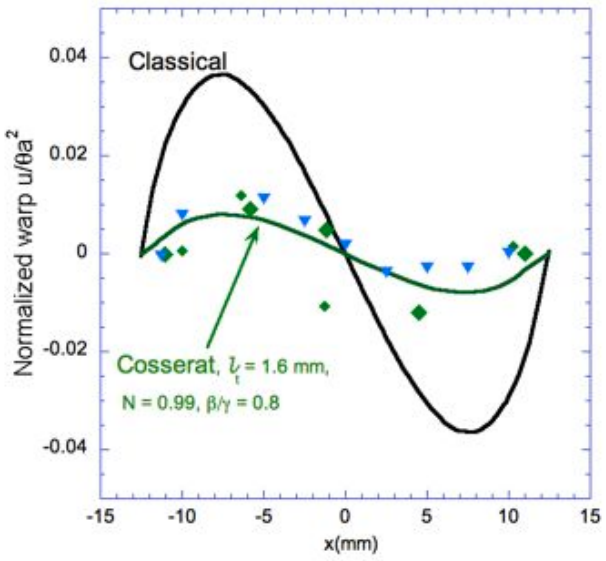

Figure 2: Warp of a foam bar in torsion; average cell size is 0.4 mm. Solid curves are theoretical for classical elasticity and Cosserat elasticity ($\ell_t = 1.6$ mm, $N = 0.99$, $\Psi = 1.5$, $\beta/\gamma = 0.8$). Points are experimental: solid diamonds, image superposition of markers; triangles, digital image correlation.

For the foam, the image superposition method disclosed too much heterogeneity of motion of surface features to extract meaningful warp deformation. Therefore, warp based on marker motion in image superposition is shown as solid diamonds in Figure 2. The inferred maximum warp displacement was about 50 μm; the pixel resolution was 10 μm.

Digital image correlation permitted averaging of local motion. Transverse scans across the surface revealed much scatter. Heterogeneity of motion was evident. Points based on averages of 100 data points in the axial (z) direction were therefore taken and results are shown as triangles in

Figure 2. Experimental foam warp magnitude is on average 31% of the classical value from marker motion and 20% of the classical value from image correlation. The prediction based on Cosserat elastic constants from size effects is a warp magnitude 22% of the classical value. Digital image correlation allows sub-pixel resolution, therefore the results are potentially more precise than results from photographic subtraction. However the correlation method does not provide a direct value of precision. Nevertheless the averaging process combined with sub-pixel resolution permits results to be obtained with sufficient quality to make inference of a large difference between observed warp and classical warp.

The maximum warp displacement, even in the classical case, is small compared with displacements associated with twist. The reason is that the warp curve undergoes two reversals over the width of the bar in contrast to the twist, Eq. 2 and 3, which is linear in axial coordinate.

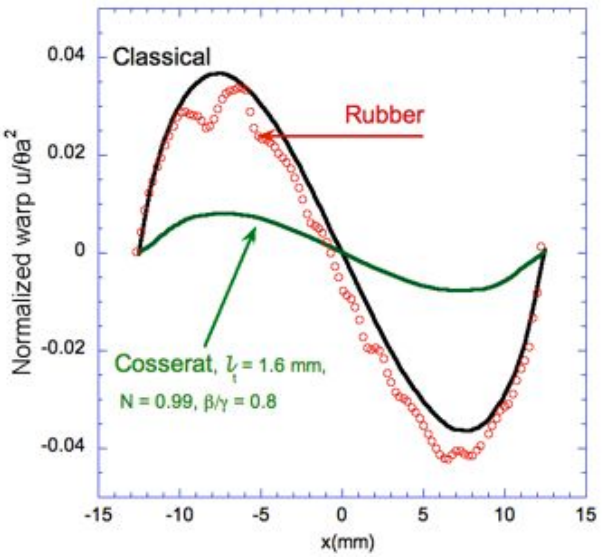

Figure 3: Warp of a rubber bar in torsion. Solid curves are theoretical for classical elasticity and Cosserat elasticity. Points (open circles) are experimental, from digital image correlation.

Warp of rubber based on digital image correlation is shown in Figure 3. The image correlation approach generates some ripples. These are attributed to the image correlation of the provided surface texture of speckles. The speckle pattern could be optimized for the rubber but since it is not possible to do so for the foam, such refinement was not pursued. The warp peak magnitude is essentially classical as is expected from the fact that the largest structure size in the rubber is that of the molecules.

Warp of the foam bar in torsion is substantially reduced (by about a factor of four) in comparison with the classical elasticity result and in reasonable agreement with the theoretical curve for Cosserat elasticity. The effect of the microstructure in this configuration is large. The foam bar is about 60 cells wide, yet the deformation differs substantially from the classical prediction.

Scatter of raw displacement values for the foam is attributed to non-affine heterogeneous deformation. Such deformation was observed in prior holographic studies [18] of copper open cell foam which has a structure similar to that of the present foams. Also, surface cells are incomplete, so protruding ribs exhibit scatter in their deformation.

The observed warp in torsion of open cell foam is substantially less than the warp predicted

by classical elasticity. The observed reduced warp is, by contrast, consistent with warp predicted from Cosserat elasticity using elastic constants based on size effect measurements. The present observation is an illustration of the predictive power of Cosserat elasticity. Reduction in warp entails a reduction in the concentration of strain which is pertinent to toughness. The present polymer foam is flexible and deforms a great deal before tearing but brittle foams (ceramic or metal) of similar structure are known [19]; for such foams, a reduction in strain concentration is expected to enhance toughness. Also, a critical stress intensity factor as a measure of toughness [20] has been shown to increase with the Cosserat characteristic length ℓ_t.

4 Conclusions

Warp in the torsion of open cell foam is substantially reduced, by about a factor of four, in comparison with the prediction of classical elasticity. Cosserat elasticity, with elastic constants obtained from prior size effect measurements, can account for the observed warp.

5 Acknowledgements

We gratefully acknowledge support of this research by the National Science Foundation via Grant CMMI-1361832.

References

[1] Sokolnikoff, I. S., *Theory of Elasticity*, Krieger; Malabar, FL, (1983).
[2] Cosserat, E. and Cosserat, F., *Theorie des Corps Deformables*, Hermann et Fils, Paris (1909).
[3] Mindlin, R. D., Stress functions for a Cosserat continuum, Int. J. Solids Structures, **1**, 265-271 (1965).
[4] Mindlin, R. D., Effect of couple stresses on stress concentrations, Experimental Mechanics, **3**, 1-7, (1963).
[5] Eringen, A. C., 1968, Theory of micropolar elasticity. In *Fracture*, **1**, 621-729 (edited by H. Liebowitz), Academic Press, New York.
[6] Park, H. C. and R. S. Lakes, Torsion of a micropolar elastic prism of square cross section. Int. J. Solids, Structures, **23**, 485-503 (1987).
[7] Anderson, W. B., Lakes, R. S., and Smith, M. C., Holographic evaluation of warp in the torsion of a bar of cellular solid, Cellular Polymers, **14**, 1-13 (1995).
[8] Lakes, R. S., Gorman, D., and Bonfield, W., Holographic screening method for microelastic solids, J. Materials Science, **20** 2882-2888 (1985).
[9] Lakes, R. S., Experimental microelasticity of two porous solids, Int. J. Solids and Structures, **22**, 55-63 (1986).
[10] Anderson, W. B. and Lakes, R. S., Size effects due to Cosserat elasticity and surface damage in closed-cell polymethacrylimide foam, J. Materials Science, **29**, 6413-6419 (1994).
[11] Mora, R. and Waas, A. M., Measurement of the Cosserat constant of circular cell polycarbonate honeycomb, Philosophical Magazine A **80**, 1699-1713 (2000).
[12] Sikon, M., Theory and experimental verification of thermal stresses in Cosserat medium, Bulletin of the Polish Academy of Sciences: Technical Sciences, **57**(2), 177 - 180, (2009)
[13] Rueger, Z. and Lakes, R. S., Experimental Cosserat elasticity in open cell polymer foam, Philos. Mag. **96** (2), 93-111, January (2016).
[14] Foamade Industries, Auburn Hills, MI.
[15] Peters, W.H., Ranson, W.F. Digital imaging techniques in experimental stress analysis. Opt. Eng. 21, 427-431 (1982).
[16] Lecompte, D.; A. Smits, S. Bossuyt, H. Sol, J. Vantomme, D. Van Hemelrijck, A. M. Habraken, Quality assessment of speckle patterns for digital image correlation, Optics and Lasers in Engineering, **44**, 1132-1145, (2006)
[17] Wang, Y., Cuitino, A. M. Full-field measurements of heterogeneous deformation patterns on polymeric foams using digital image correlation, International Journal of Solids and Structures **39** 3777-3796 (2002).
[18] Chen, C. P. and Lakes, R. S., Holographic study of non-affine deformation in copper foam with a negative Poisson's ratio -0.8, Scripta Metall et Mater., **29**, 395-399, (1993).
[19] Gibson, L. J. and Ashby, M. F., *Cellular Solids*, Pergamon, Oxford; 2nd Ed., Cambridge (1997).
[20] Radi, E. On the effects of characteristic lengths in bending and torsion on Mode III crack in couple stress elasticity, International Journal of Solids and Structures **45**, 3033-3058, (2008).